

# Design of a One-Third Scale Multi-Tethered Aerostat System for Precise Positioning of a Radio Telescope Receiver

Casey Lambert, Aaron Saunders, Curran Crawford and Meyer Nahon  
Dept. of Mechanical Engineering  
McGill University  
Montreal Quebec, Canada, H3A 2K6  
Tel: (514) 398-2383, email: Meyer.Nahon@mcgill.ca

## Abstract

The National Research Council of Canada's Herzberg Institute has proposed a design for a new radio telescope known as the 'Large Adaptive Reflector' (LAR). The LAR telescope is comprised of a 200 m reflector and a receiver held aloft at an altitude of 500 m by a tethered aerostat. The position of the receiver is actively controlled by a series of tethers connected to winching systems on the ground. Computer simulations of the LAR positioning system have shown that the proposed design holds a great deal of promise. To add confidence to these results and give further assurance that the concept is practical, experimental validation is crucial. Therefore design and construction was undertaken of a one-third-scale model of the multi-tethered aerostat component of the LAR to further study the dynamics and control of this subsystem. The design process begins with an analytical study of the scaling process. All variables liable to affect the dynamics of the system were identified and dimensionless groups were formed by applying Buckingham's Pi Theorem. Once the desired physical characteristics of the scaled system had been identified, components were chosen to satisfy those characteristics. The key components to be selected included the aerostat, tethers, sensing instruments and winches. The design process for selecting these components is discussed and an overview of the construction of the system is given.

## Introduction

In the interest of drastically improving the capabilities of current radio telescope technology, the international radio astronomy community is pursuing the development of an instrument commonly known as the square kilometre array (SKA). The instrument will be comprised of many individual radio telescopes functioning together as an array with a total of one square kilometre of collecting area. Researchers at the National Research Council of Canada's Herzberg Institute of Astrophysics have put forward a novel design concept for the SKA known as the large adaptive reflector (LAR) which is depicted in Figure 1.<sup>1-6</sup> The LAR concept consists of two central components. The first is a 200 m diameter parabolic reflector with a focal length of 500 m, composed of actuated panels supported by the ground. The second component is the receiver package which is supported by a tension structure consisting of multiple long tethers and a helium filled aerostat. Approximately 50 LAR telescopes are required to make up the square kilometre array.

The position of the receiver is controlled by changing the lengths of the tethers with winches and is performed at both macro and micro levels. At the macro level, the receiver is moved to various locations on a circular hemisphere to allow the telescope to point to different regions in the sky. For sufficient coverage of the sky, the system must be capable of positioning the receiver for a range of zenith angles from 0 to 60° ( $0 \leq \theta_{ze} \leq 60^\circ$ ) for the full range of azimuth angles ( $0 \leq \theta_{az} \leq 360^\circ$ ). Once the receiver is in place, the micro-level position control of the tethered aerostat system responds to disturbances such as wind gusts in order to limit the movement of the receiver. It is clear that the viability of the LAR concept hinges on the capacity of the tethered aerostat positioning system to limit the receiver's motion within an acceptable range.

In an earlier study, Nahon<sup>5</sup> assembled a mathematical model and simulation of the dynamics of the tethered aerostat system which yielded encouraging results of the accuracy of the positioning system. Based on the outcome of this study, a second and more detailed stage of analysis was

initiated focusing on experimental investigation of a scaled model of the tethered aerostat system. There are two important goals of the experimental study: verifying the dynamic positioning capability and determining the operational feasibility of the system. From a dynamics perspective, the goal of the scaled model is to measure the behaviour of the system in attempt to validate the dynamics model and demonstrate the accuracy of the positioning system. From an operational perspective, the goal is to use the scaled model to study the logistics and potential issues inherent in operating the tethered aerostat system. In order to satisfy both objectives, it was decided to construct the scaled system at one-third the size of the full system. This size was chosen as it is large enough to have relevance to the operation of the full scale system and it is small enough to be affordable. The tethered aerostat positioning system and the dimensions of the scaled system are shown in Figure 2.

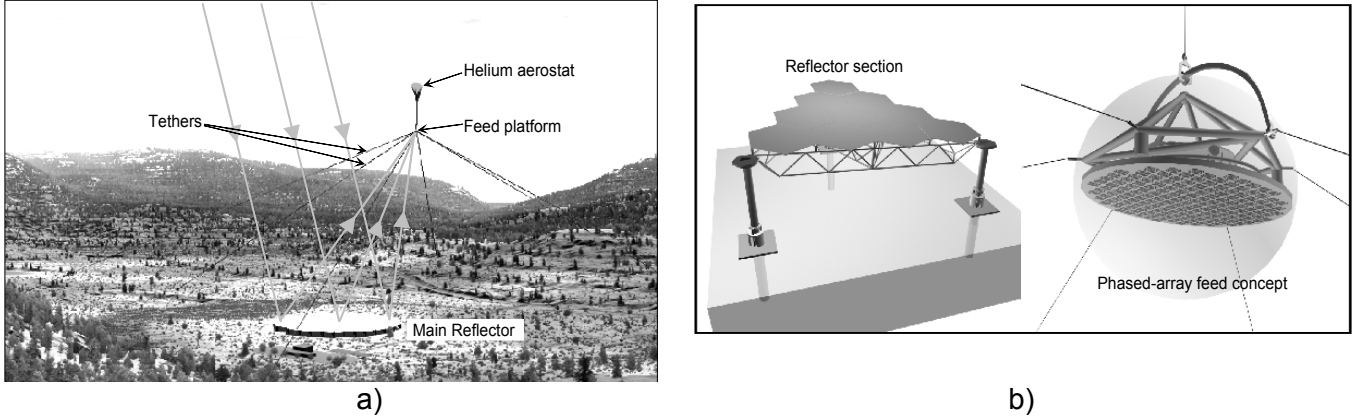


Fig. 1. a) Artist's concept of the LAR installation. b) details of one of the main reflector sections and the prime-focus phased-array feed concept.<sup>3</sup>

This paper presents the details of the design of the experimental tethered aerostat system. The design process begins with an analytical study of the scaling process for our system which involves a dimensional analysis of all variables pertinent to its dynamics. The details of the scaling process are presented along with simulation results that confirm the dynamic similarity of the scaled and actual system. Once the desired characteristics for the scaled system were identified, components were chosen to satisfy those characteristics. The key components to be selected include the aerostat, tethers, sensing instruments and winches. The design process for selecting these components is discussed and an overview of the construction of the system is given.

## Scaling Process

The technique of using a scale model to predict the performance of a large dynamical system is a common engineering practice and several methods have been developed to scale the physical parameters of the system while maintaining dynamic similarity. The method chosen for scaling the parameters of the tethered aerostat system uses the Buckingham Pi Theorem<sup>7</sup> to arrange the relevant dynamic parameters into  $n - m$  dimensionless groups. Where  $n$  is the number of dynamic variables and  $m$  is the number of fundamental dimensions used in the description of the variables.

The first step of this procedure is to identify the relevant dynamic variables, which are given in Table 1 along with their respective dimensions. From Table 1 it is observed that for our system the number of relevant parameters is  $n = 13$  and the number of fundamental dimensions is  $m = 3$  which are mass (M), length (L) and time (T). Therefore 10 dimensionless terms, referred to as  $\Pi$  terms, are required to describe the system. One possible arrangement of the dimensionless terms is:

$$\Pi_1 = \frac{m}{\rho_e l^3}, \quad \Pi_2 = \frac{J}{\rho_e l^5}, \quad \Pi_3 = \frac{F}{\rho_e U^2 l^2}, \quad \Pi_4 = \frac{\rho}{\rho_e}, \quad \Pi_5 = \frac{E}{\rho_e U^2} \quad (1a)$$

$$\Pi_6 = \frac{b}{\rho_e U l^2}, \quad \Pi_7 = \frac{\rho_e U l}{\mu}, \quad \Pi_8 = \frac{U^2}{g l}, \quad \Pi_9 = \frac{t U}{l}, \quad \Pi_{10} = \frac{f l}{U} \quad (1b)$$

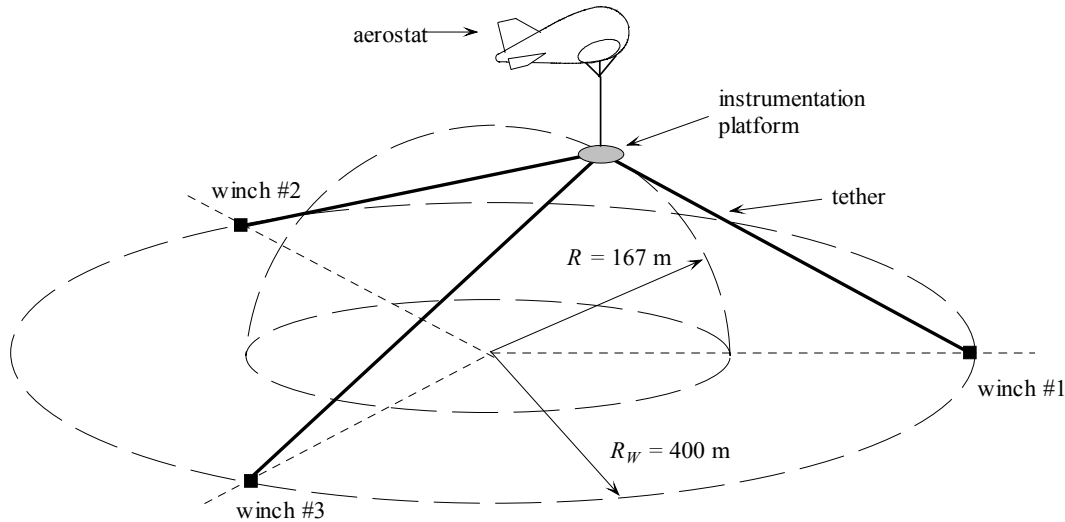


Figure 2: Tethered aerostat positioning system for 1/3 scaled system.

An inspection of the  $\Pi$  terms reveals some common dimensionless parameters:  $\Pi_7$  is Reynolds' number,  $Re$ ;  $\Pi_8$  is the Froude number,  $Fr$ , and  $\Pi_{10}$  is Stouhal's number,  $St$ . To ensure strict dynamic similarity between the model and the prototype, *all* dimensionless  $\Pi$  terms must be equal for the two systems. Using these equalities it is possible to determine the appropriate scaling factor,  $\lambda$  for each variable. The scaling factor is ratio of the scaled quantity to the actual quantity. For example the scaling factor for any length is  $\lambda_l = 1/3$ . The scaling factors for certain variables were predetermined either by the one-third scaling condition for the length or by the environmental testing conditions available. Since the scaled model and the actual system will both operate in the same outdoor environment, the scaling factor for the environmental parameters (density, viscosity, gravity) is fixed at one (i.e.,  $\lambda_{\rho_e} = \lambda_{\mu} = \lambda_g = 1$ ).

A consequence of our inability to scale the environmental conditions is that strict equality of all the dimensionless terms cannot be satisfied. A conflict arises when considering the  $\Pi_7$  and  $\Pi_8$  terms or  $Re$  and  $Fr$ . For consistent scaling of  $Re$ , the scaling factor for the velocity,  $\lambda_U = 3$ , but for consistent scaling of  $Fr$ ,  $\lambda_U = \sqrt{1/3}$ . In light of this conflict, we must decide *which* dimensionless number should be matched so as to provide closer similarity.

Table 1: Relevant parameters for tethered aerostat system.

Category	parameter	symbol	Dimension
Mechanical Components	length	$l$	L
	mass	$m$	M
	moment of inertia	$J$	$ML^2$
	force	$F$	$MLT^{-2}$
	density	$\rho$	$ML^{-3}$
	tether elastic modulus	$E$	$ML^{-1}T^{-2}$
	tether damping coefficient	$b$	$MT^{-1}$
environment	velocity	$U$	$MT^{-1}$
	density	$\rho_e$	$ML^{-3}$
	viscosity	$\mu$	$ML^{-1}T^{-1}$
	acceleration due to gravity	$g$	$LT^{-2}$
Response	time	$t$	T
	frequency	$f$	$T^{-1}$

This task is not straightforward since both dimensionless terms appear to have relevance to the aerostat system. The  $Re$  can be interpreted as a ratio of inertia forces to viscous forces while the  $Fr$  can be interpreted as the ratio of inertia forces to gravity forces. Therefore, understanding which dimensionless term is more significant can be reduced to understanding which force has a greater influence on the aerostat system, viscous forces or gravity forces. For steady fluid flow applications  $Re$  similarity is more important as gravity effects are minimal compared to their viscous counterparts. Conversely, for fluid flow applications near stream boundaries,  $Fr$  similarity is more important as gravity effects dominate over viscous forces. For the tethered aerostat system, both the gravity forces and the viscous forces are expected to influence the dynamics. To investigate this matter further, it was decided to perform a quantitative comparison of the dynamic similarity of the scaled systems with proper  $Re$  scaling and with proper  $Fr$  scaling.

Once the scaling factors for each system were determined, a previously developed simulation<sup>5</sup> was used to simulate the response of the system to a certain wind field. This simulation includes dynamics models of the tethers, aerostat and receiver. To assess the dynamic similarity, the results for each scaled system were compared to simulation results for the full scale system. To do this systematically, the input variables such as wind speed must be multiplied by the appropriate scaling factor and the output variables such as position and tether tension must be multiplied the inverse of the appropriate scaling factor. Figure 3 and 4 present these appropriately scaled simulation results for the scaled and full scale system. If the plots of the scaled and full scale system overlay, this indicates that dynamic similarity has been achieved. The plots show the vertical position error of the receiver and the tension in one of the three grounded tethers. The test case considered is one in which the open-loop (uncontrolled) system with a spherical aerostat is released from a non-equilibrium initial condition, and the wind speed is ramped up from 0 to 10 m/s between  $t = 5$  s and  $t = 6$  s.

From the results in Figures 3 and 4 it is apparent that the scaled system with  $Fr$  scaling shows much better agreement with the full scale system. This implies that the gravity forces are more significant to the dynamic behaviour of the system than the viscous forces. More significantly to our efforts, the close agreement in Figure 4 demonstrates that although it is not possible to maintain strict dynamic similarity, by maintaining  $Fr$  and ignoring  $Re$  it is nonetheless possible to accurately predict the behaviour of the actual system using a scaled model.

The physical parameters of the full scale system shown in Table 2 are based on the preliminary design of the LAR system<sup>3</sup>. It is understood that it might not be possible to find components for the scaled system that will give the precise values for the various physical parameters. For instance, a tether material may not exist that matches the specified density, elasticity and damping characteristics. This does not interfere with the goal of this study however, since the validation of the dynamics model can be performed with any tether material.

Table 2: Physical parameters for scaled model with consistent  $Fr$  scaling.

Component	Parameter	Full scale system	scaling factor	scaled system
tethers / leash	diameter	18.5 mm	$\lambda_l = 1/3$	6.17 mm
	density	840 kg/m <sup>3</sup>	$\lambda_\rho = 1$	840 kg/m <sup>3</sup>
	elastic modulus	16.8 GPa	$\lambda_E = 1/3$	5.6 Gpa
	damping coefficient	10000 kg/s	$\lambda_b = (1/3)^{2.5}$	641.5 kg/s
Aerostat	diameter	19.7 m	$\lambda_l = 1/3$	6.57 m
	mass	609.6 kg	$\lambda_m = (1/3)^3$	22.6 kg
	buoyancy	40876 N	$\lambda_F = (1/3)^3$	1514 N
receiver	diameter	6 m	$\lambda_l = 1/3$	2 m
	mass	500 kg	$\lambda_m = (1/3)^3$	18.5 kg
overall system	focal length	500 m	$\lambda_l = 1/3$	166.7 m
	winch circle radius	1200 m	$\lambda_l = 1/3$	400 m

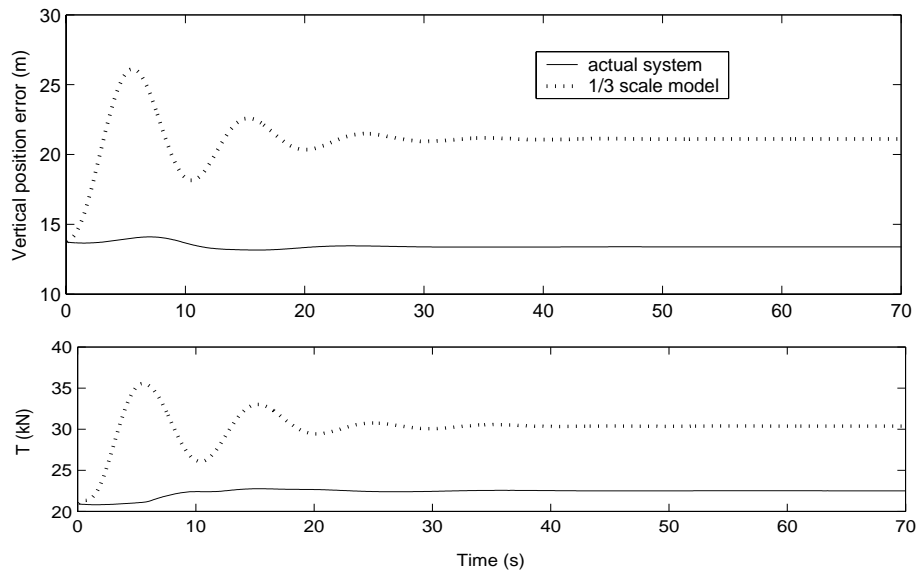


Figure 3: Simulation results; Vertical position error and tether tension, for the scaled model (dotted line) and the full scale system (solid line), using  $Re$  scaling.

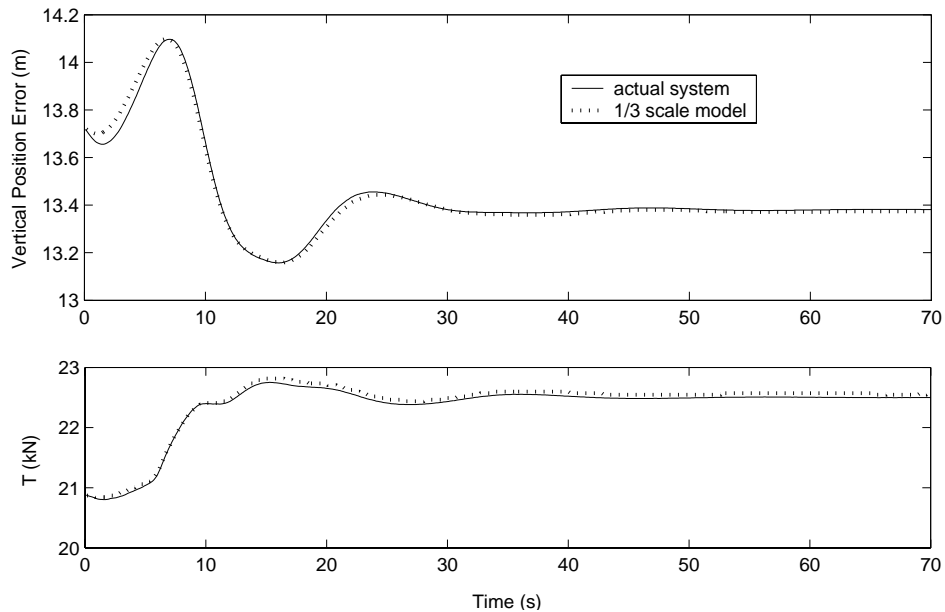


Figure 4: Simulation results; error of receiver out of the focal plane and tether tension, for the scaled model (dotted line) and the full scale system (solid line), using  $Fr$  scaling.

## System Design

The strategy for the design of the scaled experimental system was to use off the shelf parts wherever possible. The aerostat and tethers were selected based on the requirements established during the scaling process and off the shelf availability. By contrast, no commercially available winch met our requirements. The winching system therefore had to be designed in detail, based on the requirements predicted by the simulation results.

### Aerostat

A basic study of three shapes of aerostats was conducted to determine which would be most suitable for the scaled experimental system. The shapes considered were: a) spherical, b) streamlined and c) variable lift (kite). The criteria for selecting an appropriate shape for the aerostat included the following factors: aerodynamic performance, survivability, cost, availability and ground handling.

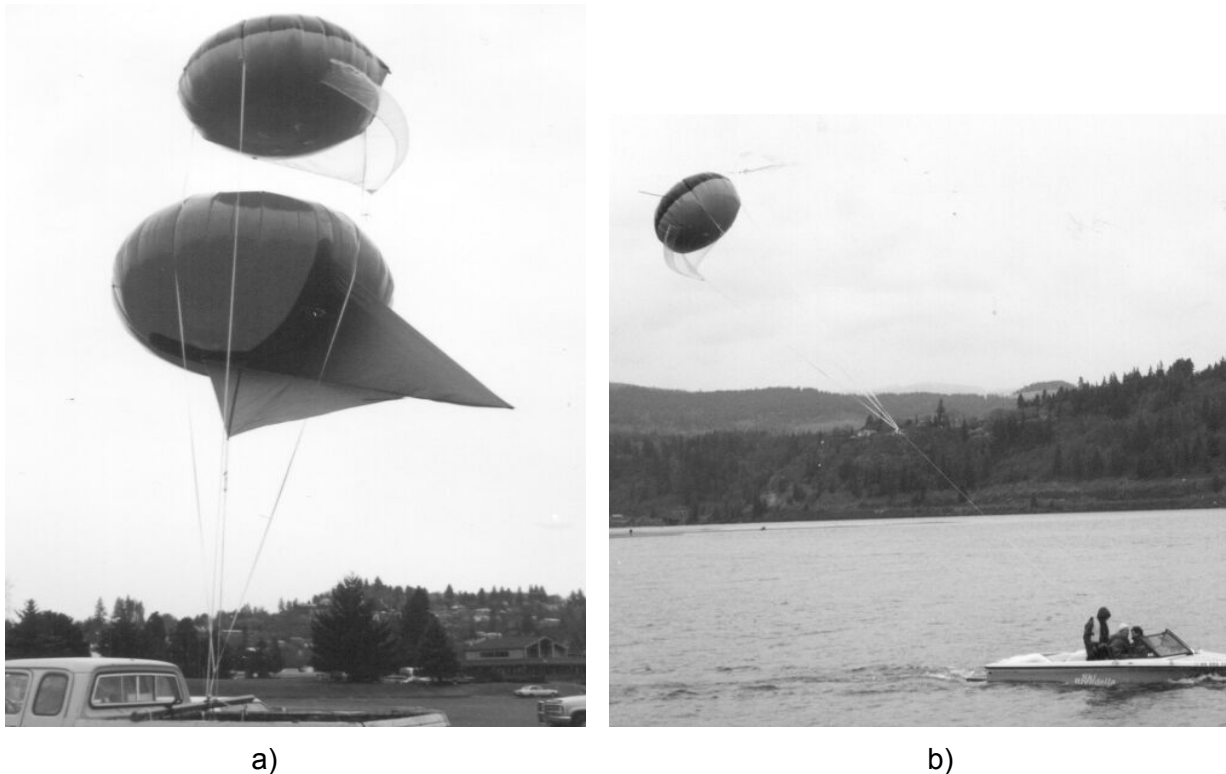


Figure 5: a) Two variable lift aerostats: Skydoc above and Helikite below, b) Testing Skydoc on the Columbia River.

The spherical aerostat, as its name implies, has a spherical shape. This is the simplest type of aerostat as it has no preference to a particular orientation and does not produce any aerodynamic lift in a horizontal wind profile. The streamlined aerostat has an aerodynamic shape like a teardrop to reduce its wind drag and a number of tail fins for directional stability. A third type of aerostat is termed variable lift reflecting its ability to generate a significant amount of lift in a wind field. The variable-lift aerostats generate lift through the addition of wings or lifting surfaces, or alternatively by simply using the hull to derive lift.

Two different variable lift aerostats, the Skydoc and Helikite were considered. Both are shown in Figure 5. The smaller aerostat on top is the Skydoc aerostat. It is an oblate (flattened) spheroid and its mesh flying harness gives it a pitched orientation which allows its hull to generate lift in a wind field. The lower aerostat is the Helikite and it is a combination of a spheroid aerostat and a kite. It generates lift using its delta wing. The attraction of such aerostats is their ability to maintain a more vertical orientation in high winds. For a conventional aerostat, only the drag increases as the wind speed increases and, as a result, the aerostat loses altitude as the angle of the aerostat tether becomes less and less vertical. To evaluate the performance of the two variable-lift aerostats, experimental tests were performed while towing the aerostats behind a boat. During the tests, poor performance of both aerostats was observed. At high speeds between 40 and 50 km/hr, the aerostats became unstable, and sometimes dove violently all the way to the water surface. Based on these observations it was decided to exclude the variable-lift aerostats from further analysis and instead focus on more conventional spherical and streamlined types.

The aerodynamic performance of the spherical aerostat is characterized by a single drag force on the hull which is proportional to its constant spherical cross section. To compare the drag coefficient of a spherical and streamlined aerostat, a reference  $Re$  of  $10^6$  was chosen which represents typical operating conditions of the scaled aerostat. The drag coefficient for a spherical body is about 0.15, while for a streamlined body of fineness ratio 2.4, it is in the approximately 0.05.<sup>8</sup> When the fins are added to the streamlined aerostat, its drag coefficient increases to 0.073. In addition to having a drag coefficient of about half that for a spherical shape, the streamlined aerostat also has a frontal area 1.7

times smaller for the same internal volume of Helium. Thus, the drag force acting on a streamlined aerostat is about 3.5 times smaller than on an equivalent spherical aerostat. The reduced drag of the streamlined aerostat has important advantages for the tethered system. From a static perspective, the loading on the tether structure would be reduced and therefore the design can be lighter and more efficient, as was reported in the original analysis of the LAR concept.<sup>3</sup> As well, the disturbances to the tether tension structure due to wind gusts should be reduced which would result in smaller position errors of the receiver. Spherical bodies also tend to be subject to vortex shedding oscillations in steady flow<sup>9</sup>. These could substantially degrade the performance of the system with a spherical aerostat. This again suggests that a streamlined aerostat may be preferable for our application as a steadier leash tension is considered desirable.

Ground handling and mooring are among the most difficult problems encountered in the operation of tethered aerostats<sup>10</sup>. The support system for handling the aerostat near or on the ground is often more complex and costly than the aerostat itself. The ground handling equipment for the streamlined aerostat must accommodate its tendency to rotate into the wind. If the aerostat is unable to rotate freely, the loading from even mild side winds is strong enough to generate very large forces. If the mooring station does not permit the aerostat to rotate freely, then it must completely shelter the aerostat from the wind. In this case, additional equipment is required to transport the aerostat from the shelter to the launch site. By contrast, the ground handling equipment for the spherical aerostat would be substantially simpler since it does not need to weathervane.

For this project, greater emphasis was placed on performance of the positioning system, and so a streamlined aerostat was selected (Figure 6). This was done with the known penalty of more complicated and costly ground handling equipment. It should be noted that, after this decision was made, further analysis revealed that the fluctuating lift generated by wind gusts on the aerostat hull may cause significant problems<sup>6</sup>. If this is indeed the case, a spherical aerostat may be re-considered.

### ***Tether Material***

The tether properties shown in Table 2 for the full scale system presume the use of *Spectra* as the tether material. This choice was made before the more advanced *Plasma* and *Vectran* materials were available on the market. Table 3<sup>3,11</sup> shows the inherent properties of these and other high strength commercial tether materials. It should be noted that the properties given are for a braided tether and thus differ from the constituent material properties. Based on the tether materials in Table 3, none fulfill our initial requirements for the scaled system (see Table 2) because a suitable tether material would need to have with the same density as *Spectra* but only one third its stiffness (characterized by its elastic modulus,  $E$ ).



Figure 6: Aeros Flightcam aerostat

Table 3: Properties for braided tethers of several materials.<sup>3,11</sup>

tether material	density, $\rho_t$ (kg/m <sup>3</sup> )	ultimate stress, $S_b$ , (GPa)	elastic modulus, $E$ , (GPa)	strength to weight, $S_b/\rho_t$ , ( $\times 10^5$ m <sup>2</sup> /s <sup>2</sup> )
Kevlar 49	1000	0.86	11	8.6
Spectra	840	0.98	17	12
Plasma	840	1.26	38	15
Vectran	1050	1.09	28	10
Steel	4400	0.71	80	1.6

If the full scale system design were to be revisited, it is likely that *Plasma* or *Vectran*, rather than *Spectra*, would be chosen as the tether material. Therefore, it would be logical to select *Spectra* for the scaled system, since its elastic modulus is a fraction that of the other two materials. Instead, for reasons of safety, a compromise was made to choose a tether material that would provide the best performance for the positioning system and the highest factor of safety. *Plasma* was therefore chosen for the scaled system as it has the highest strength to weight ratio the highest stiffness of the materials considered. As a consequence of this choice, the scaled system may not have strict dynamic similarity to the original full scale system. This is not considered to be a problem since the dynamics model can be validated irrespective of dynamic similarity.

The tether diameter for the scaled system was taken as 6 mm, which is close to the scaled value from Table 2 of 6.17 mm. The dynamics model was used to ensure that an adequate margin of safety would be maintained during testing. Two scenarios were considered: the first relates to normal operation, and the second relates to survivability. The first scenario considered the full operating range (zenith angles from 0 to 60°, azimuth angles from 0 to 360°) and a maximum wind speed of 6 m/s (approximately scaled from the full scale operational requirement of 10 m/s). The second scenario considered wind speeds up to 20 m/s (from Environment Canada data for Penticton, B.C.) with the system at a zenith angle of 0°, where tensions in the tethers are at a minimum. The maximum tensions in these two scenarios are 6.46 kN and 7.02 kN, respectively. The breaking strength of the tether corresponding to its ultimate stress of 1.26 GPa is 35.6 kN. For either scenario the margin of safety is above 5 and so the 6 mm diameter was deemed acceptable.

### **Instrument Platform**

In order to monitor environmental conditions and the performance of the system, an instrument platform was incorporated into the system at the confluence point of the tethers since this is where the receiver of the actual radio telescope would be located. The sensors are housed on a circular platform (Figure 7) which hangs freely on all three tethers using hanger fittings placed along its edge.

The onboard sensors are used to collect experimental data that can be used to compare to the simulation results. The complement of onboard instruments and their functions are as follows:

- 4 load cells – used to measure the tension in the three perimeter tethers and the leash,
- wind sensors – to measure the wind speed and wind direction,
- 2-axis tilt sensor – used to measure the tilt of the platform,
- digital compass – to measure the heading of the platform,
- differential GPS system – GPS antenna and receiver used to measure the position of the platform; a similar unit on the ground completes the differential system,
- inertial measurement unit – comprised of 3 accelerometers and 3 rate gyros to measure high-frequency motion of the platform,
- temperature probe – to measure local air temperature,
- radio modem – to transmit GPS data to the ground computer.

Additional sensors are mounted to a plate on the underside of the aerostat to measure its internal pressure and temperature, as well as its heading angle. All the sensors have analog outputs which are converted into digital RS-485 signals using A/D converter modules located on the platform. The RS-485 signals are then converted to RS-232 prior to transmission via a central tether.



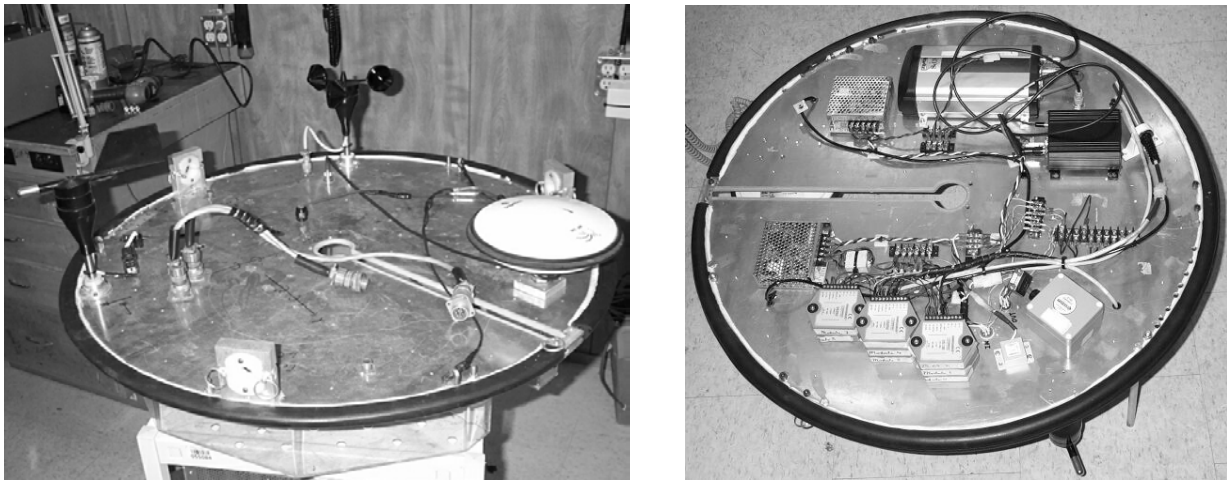


Figure 7: Top and bottom views of instrument platform.

### Winch System Design

The winch system for the scaled aerostat facility is made up of the four main components: servomotor, planetary gearbox, drum and support frame. Its design began with a determination of the required tether motion and tension, as predicted by the dynamics model. Once these requirements were established, the mechanical components were selected accordingly.

An analysis of the dynamic behaviour of the aerostat system was performed throughout its operational range in order to determine the most demanding physical configuration for the winching system. In this configuration, the zenith and azimuth angles were  $\theta_{ze} = 60^\circ$  and  $\theta_{az} = 60^\circ$ , while the wind speed and direction were 6 m/s and  $\theta_w = 150^\circ$ , respectively. The corresponding demand on each winch was quantified by the required mechanical power (tether velocity times tether tension). The details of the PID control system used for this analysis are presented by Nahon et al<sup>6</sup>. The gains used to control of the tether length were tuned so that the maximum mechanical power required was 1.5 kW---representative of the 2 kW of electrical power installed at the test site for each winch, multiplied by an estimated system efficiency of 75%. The results for the velocity, tension and power at the critical winch (Winch #1) are given in Figure 8. The resulting values for the maximum tether velocity, acceleration and tension were:  $v_{max} = 0.24$  m/s,  $a_{max} = 6.3$  m/s<sup>2</sup> and  $T_{max} = 6.14$  kN, and these were used as the basis for the design of the winch system.

The next step was to determine the requirements for the mechanical components for the winch, which are shown schematically in Figure 9. The electromagnetic torque produced by the motor,  $\tau_m$  and the motor velocity and acceleration can be estimated using the following equations:

$$\tau_m = \frac{T_{max}r}{N}, \quad \alpha_m = \frac{Na_{max}}{r}, \quad \omega_m = \frac{Nv_{max}}{r} \quad (2)$$

where  $N$  is the gear ratio and  $r$  is the tension radius of the drum.

It is clear from eq. (2) that the motor requirements depend on the gear ratio and the size of the winch drum (diameter and width). Specifically, the radial location of the tether  $r$ , is directly proportional to the required torque and inversely proportional to the speed and acceleration. For a narrow drum,  $r$  tends to be larger since the tether winds more times on the drum. Numerous combinations of drum sizes and gear ratios were investigated to minimize the required motor torque, speed and acceleration. A high gear ratio is required since the output is typically low speed and high torque.

A review of numerous motor manufacturers produced several off the shelf servosystems that could meet the requirements. The detailed requirements for the motor and gear box are given in Table 4 and 5 respectively along with the chosen components. The gearbox was selected based on having high efficiency, low inertia and low backlash. It is noted that the required gear output torque exceeds the manufacturer's continuous rating by 10%. This is not anticipated to be a problem since the peak tether load and velocity were used to determine the winch requirements.

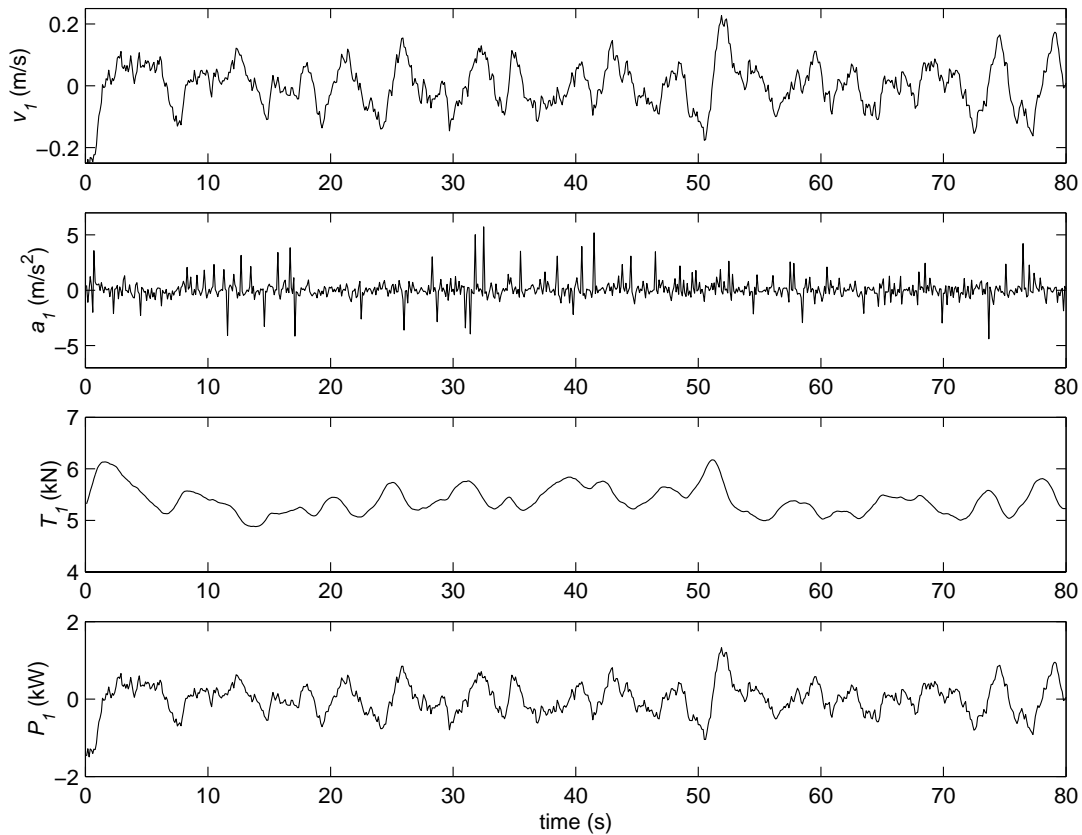


Figure 8: Tether speed, tension and power for highest power configuration for wind speed,  $U = 6$  m/s.

Once the motor and gearbox had been selected, the detailed design of the winch frame and the communication system was performed. Figure 10 a) shows the winch drum housed in its frame with the gear box. The main feature of the winch frame is the ability of the drum and drive system to rotate about a vertical axis. This feature is essential to allow the winch to accommodate the range of tether angles possible over the full operating range of motion of the receiver.

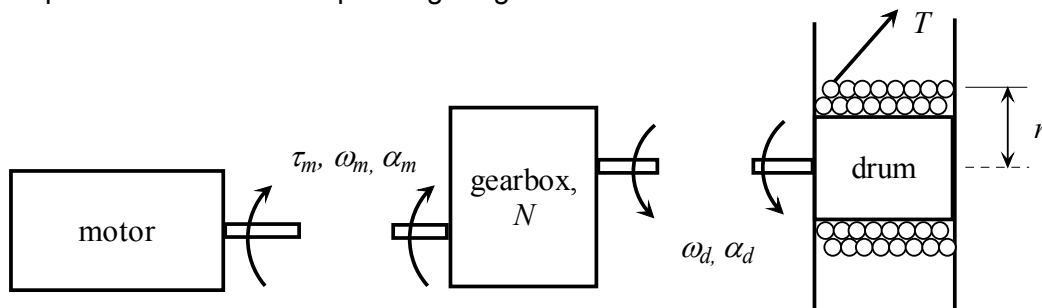


Figure 9: Mechanical components of winch system.

Figure 10 b) shows a schematic of the communication system used to transmit commands from the control computer to the winches. A PC based system was selected because of its versatility and low cost. The basic operation of the control system can be summarized as follows:

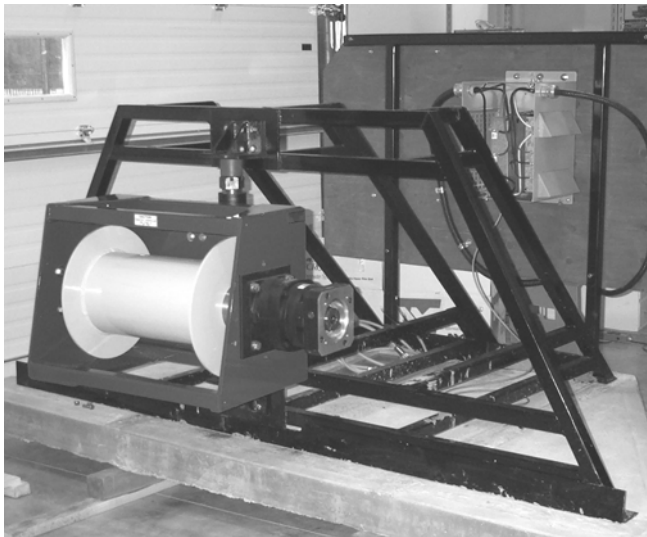
- the PC receives data from GPS and other sensors; this data is used to calculate a position error and then generate and send compensating digital commands for all winches to the motor controller (low frequency, approx. 10 Hz),
- the motor controller receives commands from the PC and issues 3 separate digital commands to the amplifier of each of the three winches (high frequency, approx. 500 Hz). The winches are connected in series by fibre optic cables and communicate in a SERCOS loop,
- the amplifier at each winch converts the control signals into the voltage and current required to drive the motor.

Table 4: Motor requirements and manufacturer's specs

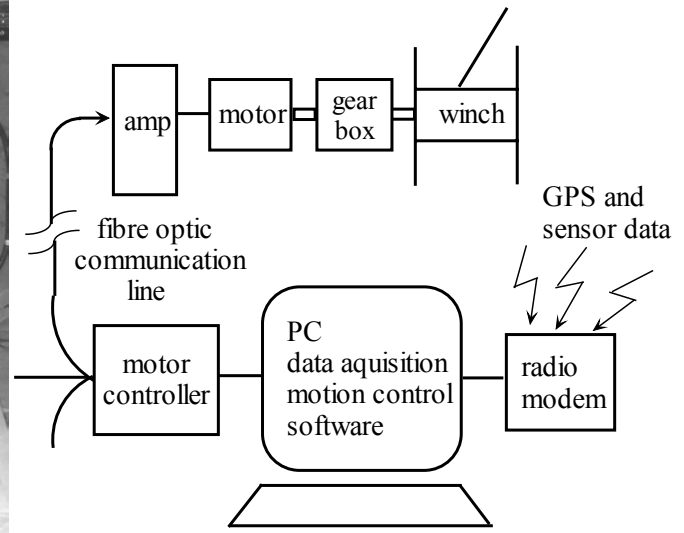
	Torque (Nm)	Speed (rpm)	Acceleration (rad/s <sup>2</sup> )
Required	11.05	1274	3502
Bosch Rexroth MHD090	12	2500	3800

Table 5: Gear box requirements and Manufacturer's specs.

	Gear Ratio	Gear Output Torque
Required	100	1105
Alpha SP210	100	1000 cont. 1520 peak



a)



b)

Figure 10: a) Winch frame with drum and gear box, b) Schematic of PC based motion control system.

### Infrastructure

A comprehensive infrastructure was constructed at the Penticton, B.C. site to support the experimental equipment. A hangar was constructed to house the aerostat when not in use, as well as a special-purpose tractor-trailer to transport the aerostat from the hangar to the launch site. These are shown in Figure 11. In addition, power and data lines were laid from the main building to the remote site and a trailer was installed to house the ground-based components including electrical junction boxes, computer, GPS system and weather station.



Figure 11: Hangar and tractor-trailer used to house and transport the aerostat.

## Conclusions

An aerostat positioning system is being investigated as the basis for a novel radio telescope design. A one third scale prototype was designed and constructed to determine the feasibility of this concept. Dimensional analysis was used to obtain the physical properties of the prototype. It was not possible to satisfy both Reynolds number and Froude number similarity. Simulation results indicated that Froude similarity was more critical in maintaining dynamic similarity to the full scale system. The results of the scaling process led to the general design specifications for scaled system. The shape of the aerostat was chosen to minimize the disturbances to the system. The selection of the tether material deviated from the properties given by the scaling process and was instead chosen for maximum stiffness and strength to weight ratio. The deviation from strict dynamic similarity should not be a problem since the validation of the dynamics model can be achieved with any tether material. In the design of the winching system, the dynamics model of the tethered aerostat system was used to estimate the required tether motion with wind speeds up to 6 m/s. The system configuration with the most power intensive requirements was identified and the resulting tether motion and tension for this case were used to establish the torque and speed specifications for the winch. Using these specifications, a suitable servomotor and gearing system was chosen.

## Acknowledgements

Funding for this research was provided by the National Research Council of Canada and by a grant from the Canada Foundation for Innovation.

## References

- <sup>1</sup>T.H. Legg. A proposed new design for a large radio telescope, *Astronomy and Astrophysics Supplement Series*, 130, pp. 369-379, 1998.
- <sup>2</sup>B. Carlson *et al.* The Large Adaptive Reflector: a 200-m diameter, wideband, cm-m wave radio telescope. *Proceedings of the SPIE International Symposium on Astronomical Telescopes and Instrumentation*, 2000.
- <sup>3</sup>J.T. Fitzsimmons, B. Veidt, P.E. Dewdney. Steady-state analysis of the multi-tethered aerostat platform for the Large Adaptive Reflector telescope. *Proceedings of the SPIE International Symposium on Astronomical Telescopes and Instrumentation*, 2000.
- <sup>4</sup>P.E. Dewdney, M. Nahon, B. Veidt. The large Adaptive Reflector: A Giant Radio Telescope with an Aero Twist. *Canadian Aeronautics and Space Journal*. Vol. 48, No. 4, pp 239-250, 2002.
- <sup>5</sup>M. Nahon. Dynamics and Control of a Novel Radio Telescope Antenna, A Collection of the *AIAA Modeling and Simulation Technologies Conference Technical Papers*, 214-222, 1999.
- <sup>6</sup>M. Nahon, G. Gilardi, C. Lambert. Dynamics/Control of a Radio Telescope Receiver Supported by a Tethered Aerostat. *Journal of Guidance, Control and Dynamics*, Vol. 25 No. 6, pp 1107-1115. 2002.
- <sup>7</sup>E. Buckingham, Model experiments and the forms of empirical equations. *Transactions. A.S.M.E.* Vol. 37, pp. 263-296, 1915.
- <sup>8</sup>B.W. McCormick. *Aerodynamics, Aeronautics and Flight Mechanics*, John Wiley & Sons, 1995.
- <sup>9</sup>R. Govardham, C.H.K. Williamson. Vortex-induced motions of a tethered sphere, *Journal of Wind Engineering and Industrial Aerodynamics*, Vol. 69, No. 71, pp. 375-385, 1987
- <sup>10</sup>S.P. Jones. Nonlinear Dynamic Simulation of a Moored Aerostat. *AIAA 7<sup>th</sup> Lighter-than-Air Technology Conference*, AIAA-87-2505, 1987.
- <sup>11</sup>Cortland Cable Company, Inc. Technical Data Sheet 105, 1987.